Article

# iBCS: 2. Mechanistic Modeling of Pulmonary Availability of Inhaled Drugs versus Critical Product Attributes

Per Bäckman,* Antonio Cabal, Andy Clark, Carsten Ehrhardt, Ben Forbes, Jayne Hastedt, Anthony Hickey, Guenther Hochhaus, Wenlei Jiang, Stavros Kassinos, Philip J. Kuehl, David Prime, Yoen-Ju Son, Simon P. Teague, Ulrika Tehler, and Jennifer Wylie

Cite This: *Mol. Pharmaceutics* 2022, 19, 2040−2047

Read Online

ACCESS | Metrics & More | Article Recommendations | SI Supporting Information

**ABSTRACT:** This work is the second in a series of publications outlining the fundamental principles and proposed design of a biopharmaceutics classifications system for inhaled drugs and drug products (the iBCS). Here, a mechanistic computer-based model has been used to explore the sensitivity of the primary biopharmaceutics functional output parameters: (i) pulmonary fraction dose absorbed ($F_{abs}$) and (ii) drug half-life in lumen ($t_{1/2}$) to biopharmaceutics-relevant input attributes including dose number (Do) and effective permeability ($P_{eff}$). Results show the nonlinear sensitivity of primary functional outputs to variations in these attributes. Drugs with Do < 1 and $P_{eff} > 1 \times 10^{-6}$ cm/s show rapid ($t_{1/2} < 20$ min) and complete ($F_{abs} > 85\%$) absorption from lung lumen into lung tissue. At Do > 1, dissolution becomes a critical drug product attribute and $F_{abs}$ becomes dependent on regional lung deposition. The input attributes used here, Do and $P_{eff}$, thus enabled the classification of inhaled drugs into parameter spaces with distinctly different biopharmaceutic risks. The implications of these findings with respect to the design of an inhalation-based biopharmaceutics classification system (iBCS) and to the need for experimental methodologies to classify drugs need to be further explored.

**KEYWORDS:** *biopharmaceutics classification system, inhaled drugs, iBCS, mechanistic modeling, critical product attributes, pulmonary availability*
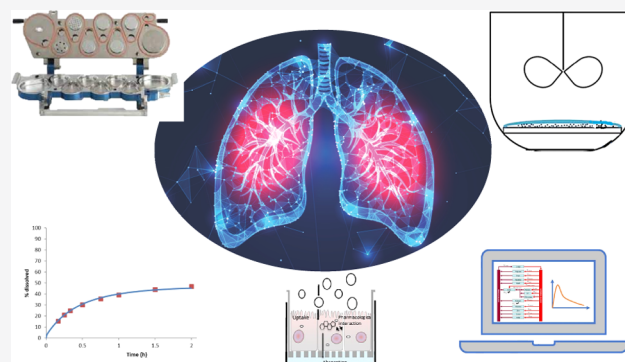
## ■ INTRODUCTION

This paper is the second in a series of publications originating from a Product Quality Research Institute (PQRI) project exploring the scientific basis and potential design of an inhalation-based Biopharmaceutics Classification System (iBCS). The potential for an iBCS was originally considered during a 2015 AAPS/FDA/USP workshop.[1] Based on the discussions from this event, it was concluded that the development of an iBCS could provide support to de-risk the development of inhaled drugs and drug products. Hence, the intent of developing an iBCS is not in the first instance to predict bioequivalence (BE) of inhaled products (since this will require in addition the development of a regulatory framework as well as the development of accepted and standardized test methods) but to help understand and mitigate product discovery and development risks. This conclusion provided the impetus for the PQRI project.

Fundamentally, an iBCS must correlate key *in vitro* attributes of a drug or drug product to a development risk or a clinical risk. The criticality of the clinical risk is determined by the sensitivity of a patient response (generally safety or drug efficacy) to variations in a key drug product attribute. As an example, the accepted biopharmaceutics classification system for orally administered drugs (giBCS) defines class 1 drugs as possessing high solubility in relation to a given dose and high permeability.[2] This ensures that giBCS class 1 drugs are rapidly and completely absorbed. Hence, *in vivo* variability caused by, e.g., factors such as variations in physiology, food intake, and formulation are lower in this class than for giBCS class 2 and 3 compounds where limited solubility and permeability, respectively, could render the rate and extent of gastrointestinal (GI) absorption susceptible to drug product and physiological variations. Fundamental to the giBCS are three dimensionless numbers, the absorption number (An, essentially the ratio of radial absorption rate to axial convection rate in the GI tract), the dissolution number (Dn, the ratio of GI residence time to
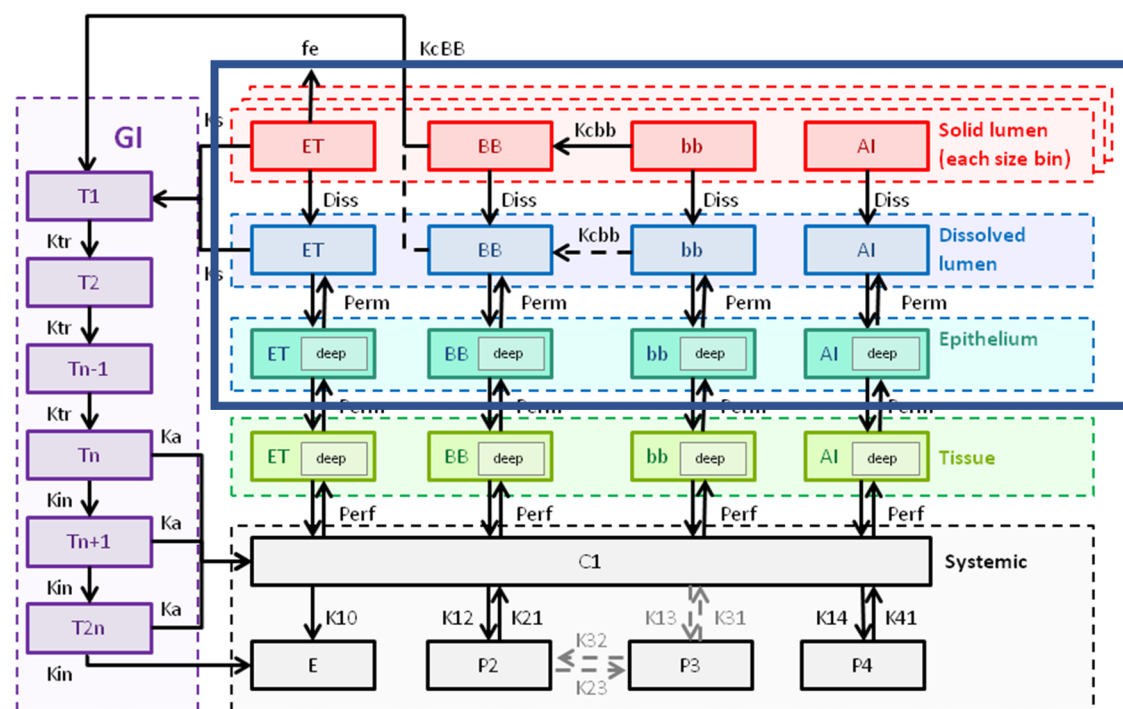
**Figure 1.** Schematic of the Mimetikos Preludium simulation model; fe = fraction exhaled, ET = mouth-throat, BB = tracheobronchial, Bb = bronchiolar, AI = alveolar interstitial, GI = gastrointestinal, C = central circulation, P = peripheral compartments, E = eliminated, T = transit compartments in GI, deep = deep compartment, Diss = dissolution of solid particles in lumen (ELF), Perm = permeation of dissolved compound over epithelium to/from lung tissue, Perf = exchange of compound between systemic circulation and lung tissue by perfusing blood, Kc = 1st-order rate constant for mucociliary transport from bb to BB ($K_{cbb}$) and from BB to 1st transit compartment ($K_{cBB}$), distributional clearance to/from deep compartment, K = 1st-order rate constant, f = fraction, F = oral bioavailability, e = expectoration/nose drip, tr and in = intercompartmental transport in GI, a = absorption from ultimate GI compartment (Tn-T2n), xx = compartment number. The solid blue box encloses processes relevant for this study.

dissolution time), and the dose number (Do, the ratio of drug dose over available fluid volume and solubility).[2] Hence, giBCS class 1 drugs are characterized by high An (>1), high Dn (>1), and low Do (<1).

There is ample evidence in the literature (see ref [1]) that the optimal properties of inhaled drugs differ significantly from those of orally ingested drugs. For example, inhaled medicines are generally developed to improve time to onset of action and safety (by directly targeting the lung).[3] Hence, desirable drug and drug product attributes should be tailored to optimize drug retention in lungs. Frequently, this results in inhaled drugs being characterized by either low solubility, low permeability, or high tissue retention, sometimes at the cost of incomplete absorption. These properties are not generally desired targets for oral drugs. Hence, it is evident that an iBCS will not have the same classifiers and classification boundaries as the giBCS. This is also true for the fundamental dimensionless numbers underpinning the giBCS. Although the Do can be adopted for an iBCS as long as modifications are made to account for the physiology of the lung airway lumen (e.g., by replacing the gastric volume in the giBCS Do with the volume of the epithelial lining fluid (ELF) in the lung), adapting the absorption number and the dissolution number is more complicated given that there is no plug flow of drug through a tube in the lung airways.[4]

The first paper in this series[4] outlined the foundational principles and framework for an iBCS. The basic hypothesis behind the adopted approach is that an iBCS can classify drugs based on the rate and extent of absorption from the airway lumen into lung tissue. It is also postulated that these functional parameters are controlled by drug and drug product attributes: solubility, dose, dissolution rate, and permeability (akin to oral drugs). Processes downstream to absorptive clearance (CL) from the luminal space, such as tissue retention and systemic disposition, are disregarded for the purposes of this work (akin to the situation for the giBCS). This is also true for processes downstream to nonabsorptive clearance from the luminal space by mucociliary clearance (MCC), i.e., absorption of the swallowed dose. However, the swallowed fraction of the dose (resulting either from direct deposition of the inhaled dose in the mouth-throat region during inhalation or by MCC from the conducting airways) may be considered orally ingested and should thus be classified according to the giBCS. Although the contribution of the orally absorbed drug fraction to the total systemic exposure must be controlled and quantified in addition to the pulmonary absorbed dose, unless the contribution is negligible (e.g., due to high first-pass metabolism or preabsorptive degradation in the GI tract), this is beyond the iBCS and thus the scope of this work.

The functional parameters controlled by an iBCS are thus proposed to be: (i) drug half-life in the luminal space of the lung ($t_{1/2,lung}$) and (ii) the fraction of the luminal dose absorbed into and across the airway epithelium ($F_{abs,lung}$). These functional parameters define the rate and extent to which the deposited drug becomes available to interact with a target in the lung tissue. This is similar to the approach adopted by the giBCS where drugs and drug products are classified with respect to their rate and extent of absorption from the GI tract. Hence, analogous to the giBCS, it would be anticipated that knowledge of the sensitivity of these functional iBCS parameters to variations in *in vitro* drug and drug product attributes could provide an understanding of key development risks and thus underpin a science-based product development strategy. To exemplify this,

a typical iBCS class 1 inhaled drug could be defined as a drug residing in a parameter space where absorption from lumen is rapid and complete, whereas iBCS class 2−4 drugs would be characterized by slower and/or incomplete absorption from lumen due to low permeability, low solubility, or both.[4] As is the case for GI absorption of oral drugs in giBCS class 2−4, assignment of inhaled drugs to these drug classes would suggest that absorption from the lung could be affected by dissolution rate (classes 2 and 4) and by variations in permeability due to drug and excipients (class 3 and 4). Obviously, the design of an inhaled drug or drug product requires consideration also of other key properties such as receptor affinity, mean residence time in lung, local and systemic tolerability, and systemic disposition. However, as discussed in paper 1 of this series,[4] descriptions of these processes require consideration of processes downstream to absorption and are thus outside the scope of an inhaled biopharmaceutics classification system.[5]

Here, the relationship between the functional output parameters ($t_{1/2,\text{lung}}$ and $F_{\text{abs,lung}}$) and the postulated key *in vitro* drug product attributes dose number (Do) (combining airway lumen initial deposited drug mass ($M_{\text{lung}}$) and drug solubility in ELF ($C_{s,\text{ELF}}$)), ELF volume, and airway drug effective permeability ($P_{\text{eff}}$) have been explored using a mechanistic computer-based model (Mimetikos Preludium). The initial drug mass used to determine the boundary between high and low solubility/dose is an input variable in the modeling. Hence, the selected approach is agnostic to the device, to the formulation properties, and to the inhalation maneuver, as discussed in paper 1 of this series.[4] Functional output parameters have been calculated using this model for *in vitro* attribute parameter ranges selected to encompass those observed for existing marketed drug products (Section B, Supporting Information).

The Mimetikos Preludium model utilized is a physiologically based pharmacokinetic (PBPK) model capable of mechanistically linking a drug or product attribute (here, solubility, permeability, and dose) to predicted and measured systemic PK response (see refs 6−9). The capability of PBPK models to provide a transparent mechanistic link between drug and drug product attributes and local lung and systemic PK makes them well-established and extensively used research tools (see refs 9−20).

## MODEL DESCRIPTION

The Mimetikos Preludium model (Mimetikos Preludium ver 1.1.7, Emmace Consulting, Lund, Sweden[6]) is schematically outlined in Figure 1. The blue box encompasses the specific parts of the model that are relevant for this study.

In the Mimetikos Preludium PBPK model, the inhaled drug is deposited in four airway regions: ET (mouth or nose); BB (tracheobronchial); bb bronchiolar; and AI (alveolar interstitial). The definition of these regions corresponds to the Weibel generations 0−8 (BB); 9−16 (bb) and 17−23 (AI).[21] Each of these regions (denoted by suffix j) is described by region-specific parametrization of epithelial surface area ($A_j$), epithelial lining fluid (ELF) depth, epithelium and tissue depths ($h_{tj}$), and the blood tissue perfusion coefficient ($Q_j$). ELF volume, epithelial tissue volume, and lung tissue volumes are determined by multiplying the surface and the respective compartment depths.

The primary functional output parameters calculated in this study are: (i) drug half-life in the luminal space of the lung ($t_{1/2,j}$) and (ii) the fraction of the luminal dose absorbed across the

airway epithelium ($F_{\text{abs,j}}$). These parameters are calculated by the model based on (i) the calculated total drug mass remaining in the ELF versus time ($t_{1/2,j}$ = the time when the drug mass in ELF is 50% of the initially deposited drug mass) and (ii) the ratio of absorptively cleared drug mass in ELF over the total drug mass deposited in ELF. Hence, none of the functional output parameters are affected by processes downstream to absorptive or nonabsorptive clearance (since $C'_{aj} \gg C'_{tj}$, eq 2 below). The functional output parameters ($t_{1/2,\text{lung}}$ and $F_{\text{abs,lung}}$) are calculated on basis of modeling the following three parallel processes.

**Dissolution of Solid Drug in Lumen.** Dissolution of polydisperse particles in the ELF takes place according to the Johnson dissolution model[22] with inputs being: calculated or measured solubility ($C_s$), diffusivity ($D_a$), and size distribution as described in eq 1

$$-\frac{dM_{ij}}{dt} = \frac{3D_a}{\rho_s h_{ij} r_{0i}} S_{0ij}^{1/3} S_{ij}^{2/3}(C_s - C'_{aj})$$

(1)

where $dM_{ij}/dt$ is the dissolution rate for size bin $i$ in region $j$, $\rho_s$ is the particle density, $r_{0i}$ is the initial particle radius, $S_{0ij}$ is the initial mass of solid, $S_{ij}$ is the remaining mass of solid, $h_{ij}$ is the diffusion layer thickness ($h_{ij} = r_{0i}(S_{ij}/S_{0ij})^{1/3}$), and $C'_{aj}$ is the free concentration in ELF.

**Absorptive Clearance from Lumen.** Once in solution, drug is absorbed over the epithelium (lost from lumen) according to the effective permeability ($P_{\text{eff}}$) value (which is an input parameter), the surface area in the region, and the free concentration gradient over the barrier[23] (eq 2).

$$-\frac{dP_j}{dt} = P_{\text{eff}_j} A_j (C'_{aj} - C'_{tj})$$

(2)

where $dP_j/dt$ is the rate of transport across the epithelium and $C'_{tj}$ is the free concentration in the subepithelium (tissue).

**Nonabsorptive Clearance from Lumen.** The mucociliary escalator transports the ELF with its solid drug content toward the pharynx where it is swallowed. This process is described by two first-order rate constants for transport from bb to BB ($K_{cbb}$) and transport from BB to the first gastrointestinal transit compartment ($K_{cBB}$), respectively.

*Model Parametrization for Sensitivity Evaluation.* To enable the simulation of rate and extent of pulmonary absorption, the Mimetikos Preludium PBPK mathematical model (essentially coupled differential equations mathematically describing processes 1−3) must be informed by (i) drug-independent parameters defining the lung physiology (Table 1) and (ii) drug-dependent parameters defining molecular properties as well as product performance attributes (Table 2). In addition, the model requires information on oral bioavailability and rate of absorption, as well as a compartmental systems PK model to convert the rate and extent of drug absorption into plasma concentrations and PK parameters such as $AUC_t$ and $C_{\text{max}}$ (Table 3).

The physiological parameters listed in Table 1 represent a Weibel-type lung model scaled to a healthy subject.[21] Similarly, epithelial lining fluid volume (ELF volume totaling 10 mL represents a conservative estimate of healthy subjects[1]). First-order rate constants ($K_{cj}$) describing mucociliary clearance (MCC) from the bronchial (bb) to the tracheobronchial region (BB) and from BB to the mouth-throat region (ET) are set to ensure that the half-life of an insoluble particle is about 1 h in the tracheobronchial region.[24]

**Table 1. Physiological Parametrization of the Mimetikos Preludium Model**

| parameter | value | source |
|---|---|---|
| definition of tracheobronchial region (BB) | generation 0−8 | 21 |
| definition of bronchiolar region (bb) | generations 9−16 | 21 |
| definition of alveolar interstitial region (AI) | generations 17−23 | 21 |
| functional residual capacity | 3000 mL | 25 |
| extra-thoracic volume | 45 mL | 25 |
| BB epithelial surface area | 0.031 m$^2$ | derived from 21 |
| bb epithelial surface area | 0.43 m$^2$ | derived from 21 |
| AI epithelial surface area | 54.7 m$^2$ | derived from 21 |
| BB epithelial lining fluid (ELF) depth | 9.7 $\mu$m | derived from volume/area |
| bb epithelial lining fluid (ELF) depth | 4.0 $\mu$m | derived from volume/area |
| AI epithelial lining fluid (ELF) depth | 0.15 $\mu$m | derived from volume/area |
| BB ELF volume | 0.3 mL | 1 |
| bb ELF volume | 1.7 mL | 1 |
| AI ELF volume | 8.0 mL | 1 |
| mucociliary (MCC) rate constant ($K_{cBB}$) | 0.69 h$^{-1}$, $t_{1/2}$, BB = 1 h | 24 |
| mucociliary (MCC) rate constant ($K_{cbb}$) | 0.078 h$^{-1}$, $t_{1/2}$, bb = 9 h | 24 |

**Table 2. Values Selected as Inputs for Testing the Sensitivity of Pulmonary Absorption to Inhaled Drug and Drug Product Attributes[a]**

| parameter | range | comment |
|---|---|---|
| molecular weight ($M_w$) | 500 g/mol | fixed value |
| diffusivity ($D$) | $3 \times 10^{-4}$ cm$^2$/min | fixed value |
| ELF solubility ($C_s$) | 0.01−10 000 $\mu$g/mL | range for sensitivity test |
| crystal density | 1 g/cm$^3$ | fixed value |
| free fraction ELF ($F_u$, ELF) | 1 | fixed value |
| lung tissue partitioning ($K_p$) | 1 | fixed value |
| epithelial permeability ($P_{eff}$) | $1 \times 10^{-5}$ to $1 \times 10^{-7}$ cm/s | range for sensitivity test |
| pulmonary region | (BB + bb) or AI | BB/bb regional split: 2:1 |
| fraction exhaled (fe) | 0 | fixed value |
| deposited dose Bb ($M_{Bb}$) | 0.2 $\mu$g−200 mg | range for sensitivity test |
| deposited dose AI ($M_{AI}$) | 0.8 $\mu$g−800 mg | range for sensitivity test |
| deposited dose lung ($M_{lung}$) | 1 $\mu$g−1000 mg | Bb/AI regional split: 4:6, 3:7 and 2:8 |
| volumetric mean diameter (VMD) | 2 $\mu$m | fixed value |
| geometric standard distribution (GSD) | 2 | fixed value |

[a]The values are typical, or encompass the range, for drugs developed as inhaled medicines.

**Table 3. Systemic PK Parameters**

| parameter | range | comment |
|---|---|---|
| oral bioavailability ($F_{po}$) | 0% | swallowed fraction from MCC |
| distribution volume ($V_d$) | 10 L | 1-compartment model |
| hepatic clearance (CL) | 80 L/h | 1-compartment model |

To investigate the fate of the inhaled drug in the lumen (i.e., drug half-life in the luminal space of the lung ($t_{1/2,lung}$) and the fraction of the luminal dose absorbed across the airway epithelium ($F_{abs,lung}$)), drug and drug product-specific parameters were selected to represent a low-molecular-weight solid drug with no tissue affinity ($K_p$ = 1, cf. Table 2). As discussed in the Introduction section, zero tissue affinity was selected to ensure that the response of outcome parameters ($t_{1/2,lung}$ $F_{abs,lung}$) to variations in key drug and drug product attributes dose ($M_j$), solubility ($C_s$), and epithelial permeability ($P_{eff}$) reflect the impact of those parameters on dissolution and passive permeation. The key drug and drug product attributes dose ($M_j$), solubility ($C_s$), and epithelial permeability ($P_{eff}$) were varied in ranges believed to encompass most pulmonary drug products on market (cf. Table B1, Supporting Information). Given the ELF volumes ($V_{ELF}$) listed in Table 1, the dose (M) and solubility ($C_s$) ranges listed in Table 2 resulted in dose numbers (Do, cf. eq 3) ranging from 0.001 to 10000. The initial dose was distributed to the region or regions of interest [sensitivity evaluations were performed for conduction airways (Bb = BB + bb), the respiratory region (AI), or the whole lung (Bb + AI)]. The distribution of dose within the conducting airways was divided BB:bb as 2:1, whereas the dose for the whole lung was divided Bb/AI as 4:6, 3:7, and 2:8 (cf. Supporting Information Section A). For the purposes of calculating dissolution rate, the polydispersity of the solid drug was set to a volumetric median diameter (VMD) of 2 $\mu$m with a GSD of 2 for all cases investigated.

In addition to the drug-specific attributes governing extent and rate of absorption, the model was also informed by a set of parameters defining oral absorption and systemic distribution and disposition (Table 3). The systemic PK model was incorporated to obtain a qualitative estimate of the impact of variations in extent and rate of pulmonary absorption on $C_{max}$ and $AUC_t$ (cf. Supporting Information Section C). In contrast to the parameters defining local absorption, these parameters do not inform a mechanistic model of systemic absorption and disposition but rather a one-compartment nonmechanistic PK model defined by distribution volume ($V_d$) and clearance (CL). Since the sensitivity work was focused on pulmonary absorption, oral bioavailability ($F_{po}$) was set to 0.

## RESULTS

The response of the primary functional output parameters ($t_{1/2,j}$ and $F_{abs,j}$) to variations in the postulated key *in vitro* drug product attributes: airway lumen initial drug mass ($M_j$), drug solubility in ELF ($C_{s,ELF}$), and airway drug effective permeability ($P_{eff}$) are shown in Figure 2. These output parameters were calculated by mechanistic computer-based modeling for the conducting airways (Bb), the alveolar interstitial region (AI), and the whole lung assuming Bb/AI ratios of 2:8, 3:7, and 4:6 (cf. Supporting Information Section C for the full data set). The response in the primary functional outputs to variations in regional dose ($M_j$) and ELF solubility ($C_{s,ELF}$) is depicted in Figure 2 as a variation with the regional dose number (Do,j) calculated according to eq 3 [4]

$$Do, j = (M_i/V_{ELF,j})/C_{s,ELF} \qquad (3)$$

The regional ELF volumes ($V_{ELF,j}$) are listed in Table 2, together with the parameter ranges for the input drug product attributes.
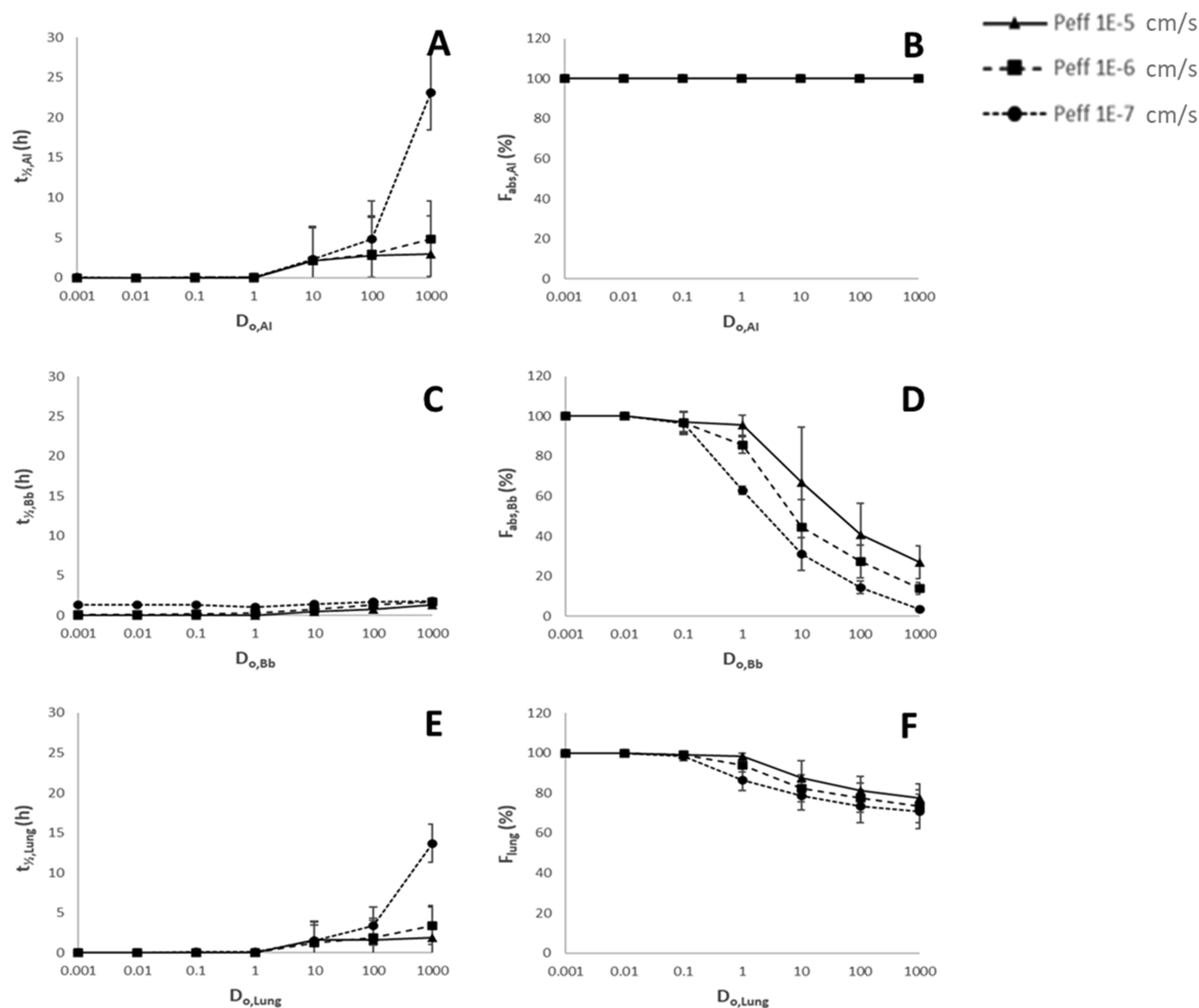
**Figure 2.** Response of calculated functional outputs luminal drug half-life ($t_{1/2,j}$) (A, C, E) and the fraction of luminal dose absorbed ($F_{abs,j}$) (B, D, F) to variation in dose numbers ($Do,j$) and permeability ($P_{eff}$) for the alveolar interstitial region (AI), (A, B), conducting airways (Bb, C, D), and total lung (E, F). Data for $P_{eff} = 1 \times 10^{-5}$ cm/s (triangles); $P_{eff} = 1 \times 10^{-6}$ cm/s (squares), and $P_{eff} = 1 \times 10^{-7}$ cm/s (circles) are shown as separate graphs in each figure. Each datapoint is the average ± SD calculated for each combination of dose and solubility resulting in a given Do. For total lung (E, F), the average ± SD also includes a variation in the Bb/AI ratio from 2:8 to 4:6 at each Do.

Results shown in Figure 2 and Table 4 indicate that an inhaled drug with a Do < 1 (i.e., the total dose is soluble in the available ELF volume) and a $P_{eff} > 1 \times 10^{-6}$ cm/s is rapidly ($t_{1/2} < 0.33$ h or 20 min) and completely ($F_{abs} > 85\%$) absorbed in all regions as well as for the total lung at dose deposition patterns (Bb/AI)

**Table 4. Primary Functional Outputs at Do = 1**

| region | $P_{eff}$ (cm/s) | $t_{1/2}$ [h (min)] | ±SD | $F_{abs}$ (%) | ±SD |
|--------|------------------|---------------------|------|---------------|------|
| Bb | $1 \times 10^{-5}$ | 0.065 (3.9) | 0.055 | 95.4 | 4.9 |
|    | $1 \times 10^{-6}$ | 0.286 (17) | 0.071 | 85.6 | 4.2 |
|    | $1 \times 10^{-7}$ | 1.042 (63) | 0.063 | 63.0 | 1.9 |
| AI | $1 \times 10^{-5}$ | 0.028 (1.7) | 0.048 | 100.0 | 0.0 |
|    | $1 \times 10^{-6}$ | 0.032 (1.9) | 0.049 | 100.0 | 0.0 |
|    | $1 \times 10^{-7}$ | 0.069 (4.1) | 0.066 | 100.0 | 0.0 |
| lung | $1 \times 10^{-5}$ | 0.035 (2.1) | 0.049 | 98.2 | 1.5 |
|    | $1 \times 10^{-6}$ | 0.053 (3.2) | 0.070 | 93.8 | 3.1 |
|    | $1 \times 10^{-7}$ | 0.113 (6.8) | 0.092 | 86.6 | 5.3 |

of 2:8; 3:7, and 4:6. As Do increases above 1, the total dose cannot be solubilized in the lumen and this, combined with lower $P_{eff}$, results in nonsink conditions, which reduce (i) the rate of absorption (here shown as an increase in luminal $t_{1/2}$, Figure 2A,C,E) and (ii) the extent of absorption (here shown as a reduction in $F_{abs}$, Figure 2D,F). The latter is not observed for the AI region (Figure 2B) since the mechanistic model is not set up to include nonabsorptive clearance (e.g., particle clearance by alveolar macrophages) from this region. The maximum value for luminal half-life in the Bb region (Figure 2C) is about 1.8 h due to mucociliary clearance (cf. Table 1), whereas the lumen half-life in the AI region can increase above 10 h at the upper end of the Do range.

The predicted increase in lumen half-life as dose number increases is generally an effect of decreased solubility on: (i) dissolution of deposited solids (cf. eq 1) and/or (ii) flux across the epithelial membrane and thus the rate of absorptive clearance from the lumen (cf. eq 2). The process that is rate-

limiting varies with the individual parametrization, the region of deposition, and the time course of the simulation, but the general observation is that sink conditions are lost in ELF as Do increases, which results in slower absorptive clearance at high doses, low solubilities, and low permeabilities. This observation is rare for the AI region due to the large absorptive surface area but more frequent in the Bb region due to a much smaller absorptive surface area (cf. Section C, Supporting Information).

## ■ DISCUSSION

The mechanistic modeling approach used herein has been widely shown to be accurate in replicating experimentally determined systemic PK resulting from pulmonary absorption (see refs 7−20). Assessing local PK in humans is more challenging due to difficulties in measuring local drug concentration, precluding the comparison of modeling outcomes with experimental data. However, using preclinical data, Boger and co-workers[10,11] have successfully linked experimental salbutamol free-drug concentrations (as estimated by target receptor occupancy) to simulated local PK providing an example where the prediction of local PK using this type of methodology was successful. Furthermore, the close correlation between calculated and systemic PK observed for fluticasone propionate [a drug with high Do, dissolution rate-limited $t_{1/2}$ and regional variation in $F_{abs}$ (cf., Table B1, Supporting Information)] observed by Bäckman and Olsson[8] suggests that the model used here is capable of accurately calculating the extent of nonabsorptive clearance (by MCC) and dissolution rate-limited absorption from the lumen. Collectively, these findings justify the use of the Mimetikos Preludium model to identify the response of primary outputs luminal half-life ($t_{1/2,j}$) and the fraction of luminal dose absorbed ($F_{abs,j}$) in lung

At Do < 1 and $P_{eff} > 1 \times 10^{-6}$ cm/s, the half-life of drug in the lumen was predicted to be short ($t_{1/2} < 20$ min) and the fraction dose absorbed was predicted to be high ($F_{abs} > 85\%$) (Table 4). This observation is true for all regions investigated (Bb and AI) and for the total lung at all investigated ratios of regional deposition (2:8; 3:7, and 4:6). Hence, drugs within this parameter space (Do < 1 and $P_{eff} > 1 \times 10^{-6}$ cm/s) are likely to have biopharmaceutics properties akin to those of giBCS class 1 drugs. Drugs within this parameter space could thus be candidates for an iBCS class 1. The absorption of drugs classified as iBCS class 1 is not likely to be significantly limited by the dissolution of inhaled solids, nor is the fraction dose absorbed likely to be significantly affected by variations in dose or regional deposition (although the latter may lead to variations in local tissue levels throughout the lung). This has implications for drug product development as changes to drug solid state prior to pivotal clinical studies may be expected to have limited clinical impact.

As with the approach used to identify the high/low permeability class boundary in the giBCS, the modeling used to determine the iBCS permeability boundary excludes lysosomal trapping, receptor site binding, general tissue interactions, and the effect of charge.[5] Many soluble inhaled drugs have a high affinity for lung tissue and are thus retained in the lung after absorption for an extended time.[3] Hence, the classification of an inhaled drug as iBCS class 1 following the above definition (Do < 1 and $P_{eff} > 1 \times 10^{-6}$ cm/s) does not infer that they are necessarily absorbed rapidly into the systemic circulation.

Drugs with Do > 1 may display dissolution limited absorption *in vivo*. Although the slow dissolution of poorly soluble drugs with Do's > 1 contributes to their retention in the lung and thus to an increased duration of therapeutic effect,[3] this desirable property may come at the cost of increased technical development risk. For instance, dissolution now becomes an important drug attribute and should be controlled in order to control absorption rate. As shown by Rohrschneider et al.,[26] Bäckman and Olsson,[8] and Bäckman et al.,[14] an *in vitro in vivo* relationship (IVIVR) can be established between *in vitro* dissolution and PK, but this requires careful consideration with regard to test methods and their *in vivo* relevance. Although a variety of dissolution test methods have been developed, there is not yet a standard pharmacopeial dissolution method for inhaled drug products. Another concern for slowly dissolving drugs may be that lung retention and thus PK and potentially pharmacological and toxicological findings during preclinical development are affected by species differences in non-absorptive clearance, drug solid state, and/or regional species-induced variations in $D_o$'s.[3,27] Furthermore, variations in dose deposition caused by differences in aerosol administration systems or by disease-induced changes to airway morphology (e.g., airway narrowing in asthma) could render the translation of PK and pharmacodynamic data between species and between healthy human subjects and patients more complex for drugs with high Do. At Do > 1, and especially in combination with $P_{eff}$ at or below $1 \times 10^{-7}$ cm/s, $F_{abs}$ is expected to be reduced in the conducting airways due to mucociliary clearance of solid drug, thus reducing overall pulmonary bioavailability (cf. Figure 2). Slow dissolution under nonsink conditions is the primary mechanistic explanation for this observation.[7,8] Hence, drugs with high Do and $F_{abs} < 1$ (e.g., neutral glucocorticosteroids)[1] are likely to display changes in $F_{abs}$ with variations in deposition pattern.[28−30] This has also been observed in clinical studies, for example, the bioavailability of fluticasone propionate was found to be significantly reduced in asthmatics compared to healthy volunteers, presumably due to an increase in Bb deposition caused by the narrowing of conducting airways in asthmatics.[31,32] Hence, species-, disease-, and product-induced variations in Do, as well as formulation-induced variations in dissolution rate, should be carefully considered when Do > 1 as it may affect local and systemic PK and thus complicate the translation between preclinical data sets, early clinical data sets in healthy subjects, and later clinical data sets in patient populations.

The response of secondary PK output parameters ($AUC_{0-t}$, $AUC_{0-inf}$, $t_{max}$, and $C_{max}$) to variations in dose numbers ($Do_j$) and permeability ($P_{eff}$) for conducting airways (Bb), alveolar interstitial region (AI), and total lung (Th) was also determined (cf. Section C, Supporting Information). However, since the sensitivity of these parameters depends on other processes such as drug tissue interactions and systemic disposition not included in this model, the secondary PK outputs are indicative at best.

The physiological parametrization listed in Table 1 is regarded to be representative of the anatomy and physiology of a typical adult subject. Obviously, variation in factors such as lung volume will influence other parameters such as epithelial surface areas and epithelial volumes which in turn will affect Do. Given that the observed variation in functional outputs ($t_{1/2}$ and $F_{abs}$) is minor at Do < 1, it would require an extreme reduction in lung volume to significantly affect the conclusions drawn above. To exemplify the effect on Do, log Do will increase from 1 to 1.3 if the lung volume is reduced to 50% of the value given in Table 1 (roughly 2.5% of the population is expected to have a lung volume ≤ 50% of the median volume based on data obtained by

Christou et al.[33]), nor will variations in MCC due to disease and/or age affect the total bioavailability of drugs that dissolve readily (Do < 1).

To limit the data set, some product attributes such as VMD (GSD), crystal density, and free fraction of dissolved drug in ELF were set to fixed values. Variation in these values resulting from drug molecular properties, solid state, and manufacturing processes will affect the dissolution rate that will in turn affect dissolution modeled outcomes for drugs with Do≫1, i.e., dissolution rate-limited drugs. However, for drugs with Do < 1, the modeling outcomes are insensitive to realistic variations in these parameters, and they are therefore not critical for the purpose of defining a class boundary between dissolution rate-limited and non-dissolution rate-limited drug products.

In summary, the observations made in this mechanistic modeling study support that drugs residing within different parameter spaces could be associated with different product development risks. Hence, classifying drugs in accordance with where they reside within the investigated parameter spaces could provide useful information and input to strategies for product performance control and translational science. In addition, the results here suggest that Do (as calculated using ELF volumes according to eq 3) and $P_{eff}$ could be candidates for classifying drugs and drug products into useful risk-based parameter spaces or iBCS classes. The implications of these findings in terms of the design of a biopharmaceutics classification system for inhaled drug products (an iBCS), as well as the need for experimental methods to establish drug classifiers and characterize inhaled drug products will need to be explored further.

## ■ ASSOCIATED CONTENT

### ⓢ Supporting Information

The Supporting Information is available free of charge at https://pubs.acs.org/doi/10.1021/acs.molpharmaceut.2c00112.

> Lung deposition patterns as a function of inhalation flow and aerodynamic particle size; dose, solubility, and effective pulmonary permeability for some marketed drug products (PDF)

> All model inputs and outputs for all conditions explored (XLSX)

## ■ AUTHOR INFORMATION

### Corresponding Author

**Per Bäckman** − *Emmace Consulting AB, Lund SE-223 81, Sweden;* ⓞ orcid.org/0000-0001-6210-8461; Phone: +46 722 497901; Email: Per@emmace.se

### Authors

**Antonio Cabal** − *Eisai, Woodcliff Lake, New Jersey 07677, United States*

**Andy Clark** − *Aerogen Pharma, San Mateo, California 94402, United States*

**Carsten Ehrhardt** − *Trinity College Dublin, Dublin 2, Ireland*

**Ben Forbes** − *King's College London, London WC2R 2LS, U.K.;* ⓞ orcid.org/0000-0001-8193-6107

**Jayne Hastedt** − *JDP Pharma Consulting, San Carlos, California 94070, United States;* ⓞ orcid.org/0000-0002-1784-4635

**Anthony Hickey** − *University of North Carolina at Chapel Hill, Chapel Hill, North Carolina 27599, United States; RTI*

*International, Research Triangle Park, North Carolina 27709, United States*

**Guenther Hochhaus** − *University of Florida, Gainesville, Florida 32611, United States*

**Wenlei Jiang** − *Center for Drug Evaluation and Research, Office of Generic Drugs, Office of Research and Standards, U.S. FDA, Silver Spring, Maryland 20993, United States*

**Stavros Kassinos** − *University of Cyprus, Nicosia 1678, Cyprus*

**Philip J. Kuehl** − *Lovelace Biomedical, Albuquerque, New Mexico 87108, United States;* ⓞ orcid.org/0000-0002-7567-3002

**David Prime** − *Pulmonary Drug Delivery Consultant, Ware SG12, U.K.*

**Yoen-Ju Son** − *Genentech, South San Francisco, California 94080, United States*

**Simon P. Teague** − *GlaxoSmithKline, Stevenage SG1 2NY, U.K.*

**Ulrika Tehler** − *Advanced Drug Delivery, Pharmaceutical Sciences, R&D, AstraZeneca, Gothenburg 43183, Sweden*

**Jennifer Wylie** − *Merck & Co., Inc., Kenilworth, New Jersey 07033, United States*

Complete contact information is available at:
https://pubs.acs.org/10.1021/acs.molpharmaceut.2c00112

### Notes

The authors declare no competing financial interest.

## ■ ACKNOWLEDGMENTS

## ■ LIST OF ABBREVIATIONS

Al, Alveoli and alveolar ducts, generations 17−23; APSD, Aerodynamic Particle Size Distribution; Bb, The central airways, generations 0−16; BE, Bioequivalence; CF, Coarse Fraction, fraction deposited in the mouth-throat; C/P, Central to Peripheral deposition pattern; ELF, Epithelial Lining Fluid; $F_{abs}$, Fraction of the dose absorbed from the lungs; giBCS, Gastrointestinal Biopharmaceutics Classification System; GSD, Geometric Standard Deviation; iBCS, Inhalation-based Biopharmaceutics Classification System; IR, Immediate Release; MMAD, Mass Median Aerodynamic Diameter; PBPK, Physiologically Based Pharmacokinetics; $P_{eff}$, Effective epithelial permeability; PQRI, Product Quality Research Institute; VMD, Volume Median Diameter

## ■ REFERENCES

(1) Hastedt, J. E.; Bäckman, P.; Clark, A. R.; Doub, W.; Hickey, A.; Hochhaus, G.; Kuehl, P. J.; Lehr, C.-M.; Mauser, P.; McConville, J.; Niven, R.; Sakagami, M.; Weers, J. G. Scope and relevance of a pulmonary biopharmaceutical classification system AAPS/FDA/USP

Workshop March 16-17th, 2015 in Baltimore, MD. *AAPS Open* **2016**, *2*, 286−295.

(2) Amidon, G. L.; Lennernäs, H.; Shah, V. P.; Crison, J. R. A. Theoretical Basis for a Biopharmaceutical Drug Classification: The Correlation of in Vitro Drug Product Dissolution and in Vivo Bioavailability. *Pharm. Res.* **1995**, *12*, 413−420.

(3) Bonn, B.; Perry, M. The API. In *Inhaled Medicines—Optimizing Development through Integration of In Silico, In Vitro and In Vivo Approaches*, Kassinos, S.; Bäckman, P.; Conway, J.; Hickey, A. J., Eds.; Elsevier Inc., 2021; pp 13−34.

(4) Hastedt, J. E.; Bäckman, P.; Cabal, A.; Clark, A.; Ehrhardt, C.; Forbes, B.; Hickey, A. J.; Hochhaus, G.; Jiang, W.; Kassinos, S.; Kuehl, P.; Prime, D.; Son, Y-J.; Teague, S.; Tehler, U.; Wylie, J. The iBCS: 1. Principles and Framework of an Inhalation-Based BCS *Mol. Pharmaceutics*, in press, DOI: 10.1021/acs.molpharmaceut.2c00113.

(5) Zur; Moran; Gasparini, M.; Wolk, O.; Amidon, G. L.; Dahan, A. The Low/High BCS Permeability Class Boundary: Physicochemical Comparison of Metoprolol and Labetalol. *Mol. Pharmaceutics* **2014**, *11*, 1707−1714.

(6) Olsson, B.; Bäckman, P. Mimetikos Preludium: A New Pharma-friendly Aerosol Drug Deposition Calculator. In *Respiratory Drug Delivery*, Dalby, R. N.; Peart, J., Eds.; Davis Healthcare International Publishing, LLC, 2018; Vol. *1*, pp 103−112.

(7) Bäckman, P.; Olsson, B. De-risking Inhalation Product Development Using Predictive Model. In *Respiratory Drug Delivery Asia*, Dalby, R. N.; Peart, J., Eds.; Davis Healthcare International Publishing, LLC: Kerela, 2018; pp 83−92.

(8) Bäckman, P.; Olsson, B. Pulmonary Drug Dissolution, Regional Retention and Systemic Absorption: Understanding their interactions though Mechanistic Modelling. In *Respiratory Drug Delivery*, Byron, P. R., Ed.; Davis Healthcare International Publishing: River Grove, Illinois, US, 2020; pp 113−22.

(9) Himstedt, A.; Bäckman, P.; Borghardt, J. M. Physiologically-Based Pharmacokinetic Modelling after Drug Inhalation. In *Inhaled Medicines—Optimizing Development through Integration of In Silico, In Vitro and In Vivo Approaches*, Kassinos, S.; Bäckman, P.; Conway, J.; Hickey, A. J., Eds.; Elsevier Inc., 2021; pp 13−34.

(10) Boger, E.; Fridén, M. Physiologically Based Pharmacokinetic/Pharmacodynamic Modeling Accurately Predicts the Better Broncho-dilatory Effect of Inhaled Versus Oral Salbutamol Dosage Forms. *J. Aerosol Med. Pulm. Drug Delivery* **2019**, *32*, 1−12.

(11) Boger, E.; Evans, N.; Chappell, M.; Lundqvist, A.; Ewing, P.; Wigenborg, A.; Fridén, M. Systems Pharmacology Approach for Prediction of Pulmonary and Systemic Pharmacokinetics and Receptor Occupancy of Inhaled Drugs. *CPT: Pharmacometrics Syst. Pharmacol.* **2016**, *5*, 201−210.

(12) Borghardt, J. M.; Weber, B.; Staab, A.; Kloft, C. Pharmacometric Models for Characterizing the Pharmacokinetics of Orally Inhaled Drugs. *AAPS J.* **2015**, *17*, 853−870.

(13) Bäckman, P.; Arora, S.; Couet, W.; Forbes, B.; de Kruijf, W.; Paudel, A. Advances in experimental and mechanistic computational models to understand pulmonary exposure to inhaled drugs. *Eur. J. Pharm. Sci.* **2018**, *113*, 41−52.

(14) Bäckman, P.; Tehler, U.; Olsson, B. Predicting Exposure after Oral Inhalation of the Selective Glucocorticoid Receptor Modulator, AZD5423, Based on Dose, Deposition Pattern, and Mechanistic Modeling of Pulmonary Disposition. *J. Aerosol Med. Pulm. Drug Delivery* **2017**, *30*, 108−117.

(15) Cabal, A.; Jajamovich, G.; Przekwas, A. In *Using Multiscale Mechanism Based Mathematical Modeling to Address Many of the Challenges Associated with the Estimation of Local Lung Concentration after Inhaled Drug Delivery*, Annual Meeting of the Population Approach Group in Europe. ISSN 1871-6032, 2019; Abstract 8810; Stockholm, Sweden, 2019.

(16) Cabal, A.; Mehta, K.; Guo, P.; Przekwas, A. In *In-Silico Lung Modeling Platform for Inhaled Drug Delivery*, Proceedings Drug Delivery to the Lungs, 2016; pp 82−86.

(17) Caniga, M.; Cabal, A.; Mehta, K.; Ross, D. S.; Gil, M. A.; Woodhouse, J. D.; Eckman, J.; Naber, J. R.; Callahan, M. K.; Goncalves, L.; Hill, S. E.; McLeod, R. L.; McIntosh, F.; Freke, M. C.; Visser, S. A. G.; Johnson, N.; Salmon, M.; Cicmil, M. Preclinical Experimental and Mathematical Approaches for Assessing Effective Doses of Inhaled Drugs, Using Mometasone to Support Human Dose Predictions. *J. Aerosol Med. Pulm. Drug Delivery* **2016**, *29*, 362−377.

(18) Chaudhuri, S. R.; Lukacova, V. Simulating Delivery of Pulmonary (and intranasal) Aerosolized Drugs, Orally Inhaled & Nasal Drug Products, 2010. www.ondrugdelivery.com, https://www.ondrugdelivery.com/wp-content/uploads/2018/11/Nov2010.pdf (accessed April 22, 2022).

(19) Weber, B.; Hochhaus, G. A pharmacokinetic simulation tool for inhaled corticosteroids. *AAPS J.* **2013**, *15*, 159−171.

(20) Weber, B.; Hochhaus, G. A Systematic Analysis of the Sensitivity of Plasma Pharmacokinetics to Detect Differences in the Pulmonary Performance of Inhaled Fluticasone Propionate Products Using a Model-Based Simulation Approach. *AAPS J.* **2015**, *17*, 999−1010.

(21) Weibel, E. R. *Morphometry of the Human Lung*; Springer: Berlin, 1963.

(22) Lu, A. T. K.; Frisella, M. E.; Johnson, K. C. Dissolution modeling: factors affecting the dissolution rates of polydisperse powders. *Pharm. Res.* **1993**, *10*, 1308−1314.

(23) Fick, A. (1855). ″On liquid diffusion″. Annalen der Physik und Chemie. 94: 59. − reprinted in Fick, Adolph. ″On liquid diffusion″. *J. Membr. Sci.* **1995**, *100*, 33−38.

(24) Agnew, J. E.; Sutton, P. P.; Pavia, D.; Clarke, S. W. Radioaerosol assessment of mucociliary clearance: towards definition of a normal range. *Br. J. Radiol.* **1986**, *59*, 147−151.

(25) International Commission on Radiological Protection (ICRP). *Human Respiratory Tract Model for Radiological Protection*; International Commission on Radiological Protection [By] Pergamon, 1994; Vol. *24*, pp 1−120.

(26) Rohrschneider, M.; Bhagwat, S.; Krampe, R.; Michler, V.; Breitkreutz, J.; Hochhaus, G. Evaluation of the Transwell System for Characterization of Dissolution Behavior of Inhalation Drugs: Effects of Membrane and Surfactant. *Mol. Pharmaceutics* **2015**, *12*, 2618−2624.

(27) Forbes, B.; O'Lone, R.; Allen, P. P.; Cahn, A.; Clarke, C.; Collinge, M.; Dailey, L. A.; Donnelly, L. E.; Dybowski, J.; Hassall, D.; Hildebrand, D.; Jones, R.; Kilgour, J.; Klapwijk, J.; Maier, C. C.; McGovern, T.; Nikula, K.; Parry, J. D.; Reed, M. D.; Robinson, I.; Tomlinson, L.; Wolfreys, A. Challenges for inhaled drug discovery and development: induced alveolar macrophage responses. *Adv. Drug Delivery Rev.* **2014**, *71*, 15−33.

(28) Burmeister Getz, E.; Carroll, K. J.; Jones, B.; Benet, L. Z. Batch-to-Batch Pharmacokinetic Variability Confounds Current Bioequivalence Regulations: A Dry Powder Inhaler Randomized Clinical Trial. *Clin. Pharmacol. Ther.* **2016**, *100*, 223−231.

(29) Burmeister Getz, E.; Carroll, K. J.; Mielke, J.; Benet, L. Z.; Jones, B. Between-Batch Pharmacokinetic Variability Inflates Type I Error Rate in Conventional Bioequivalence Trials: A Randomized Advair Diskus Clinical Trial. *Clin. Pharmacol. Ther.* **2017**, *101*, 331−340.

(30) Hastedt, J. E.; Burmeister Getz, E. Chapter 31: Bioequivalance of Orally Inhaled Drug Products: Challenges and Opportunities. In *Pharmaceutical Inhalation Aerosol Technology*, 3rd ed.; Hickey, A. J.; da Rocha, S. R. P., Eds.; CRC Press, Taylor & Francis Group: Boca Raton, FL, 2017; pp 687−717.

(31) Brutsche, M. H.; Carlen Brutsche, I.; Munavvar, M.; Langley, S. J.; Masterson, C. M.; Daley-Yates, P. T.; Brown, R.; Custovic, A.; Woodcock, A. Comparison of pharmacokinetics and systemic effects of inhaled fluticasone propionate in patients with asthma and healthy volunteers: a randomised crossover study. *Lancet* **2000**, *356*, 556−561.

(32) Harrison, T. W.; Tattersfield, A. E. Plasma concentrations of fluticasone propionate and budesonide following inhalation from dry powder inhalers by healthy and asthmatic subjects. *Thorax* **2003**, *58*, 258−260.

(33) Christou, S.; Chatziathanasiou, T.; Angeli, S.; Koullapis, P.; Stylianou, F.; Sznitman, J.; Guo, H. H.; Kassinos, S. Anatomical variability in the upper tracheobronchial tree: sex-based differences and implications for personalized inhalation therapies. *J. Appl. Physiol.* **2021**, *130*, 678−707.